

Article

Measurement on Diffusion Coefficients and Isotope Fractionation Factors by a Through-Diffusion Experiment

Takuma Hasegawa ^{1,*}, Kotaro Nakata ¹ and Rhys Gwynne ²

¹ Civil Engineering Research Laboratory, Central Research Institute of Electric Power Industry, Abiko, Chiba 270-1194, Japan; k-nakata@criepi.denken.or.jp

² Environmental Isotope Laboratory, University of Waterloo, Waterloo, ON N2L 3W8, Canada; rgwynne@uwaterloo.ca

* Correspondence: t-hase@criepi.denken.or.jp

Abstract: For radioactive waste disposal, it is important that local groundwater flow is slow as groundwater flow is the main transport medium for radioactive nuclides in geological formations. When the groundwater flow is very slow, diffusion is the dominant transport mechanism (diffusion-dominant domain). Key pieces of evidence indicating a diffusion-dominant domain are the separation of components and the fractionation of isotopes by diffusion. To prove this, it is necessary to investigate the different diffusion coefficients for each component and the related stable isotope fractionation factors. Thus, in this study, through-diffusion and effective-porosity experiments were conducted on selected artificial materials and natural rocks. We also undertook measurements relating to the isotope fractionation factors of Cl and Br isotopes for natural samples. For natural rock samples, the diffusion coefficients of water isotopes (HDO and H₂¹⁸O) were three to four times higher than those of monovalent anions (Cl⁻, Br⁻ and NO₃⁻), and the isotope fractionation factor of ³⁷Cl (1.0017–1.0021) was slightly higher than that of free water. It was experimentally confirmed that the isotope fractionation factor of ⁸¹Br was approximately 1.0007–1.0010, which is equivalent to that of free water. The enrichment factor of ⁸¹Br was almost half that of ³⁷Cl. The effective porosity ratios of HDO and Cl were slightly different, but the difference was not significant compared to the ratio of their diffusion coefficients. As a result, component separation was dominated by diffusion. For artificial samples, the diffusion coefficients and effective porosities of HDO and Cl were almost the same; it was thus difficult to assess the component separation by diffusion. However, isotope fractionation of Cl and Br was confirmed using a through-diffusion experiment. The results show that HDO and Cl separation and isotope fractionation of Cl and Br can be expected in diffusion-dominant domains in geological formations.

Keywords: diffusion-dominant; ³⁷Cl; ⁸¹Br; isotope fractionation; component separation



check for updates

Citation: Hasegawa, T.; Nakata, K.; Gwynne, R. Measurement on Diffusion Coefficients and Isotope Fractionation Factors by a Through-Diffusion Experiment. *Minerals* **2021**, *11*, 208. <https://doi.org/10.3390/min11020208>

Academic Editor: Hans Eggenkamp

Received: 17 December 2020

Accepted: 9 February 2021

Published: 16 February 2021

Publisher's Note: MDPI stays neutral with regard to jurisdictional claims in published maps and institutional affiliations.



Copyright: © 2021 by the authors. Licensee MDPI, Basel, Switzerland. This article is an open access article distributed under the terms and conditions of the Creative Commons Attribution (CC BY) license (<https://creativecommons.org/licenses/by/4.0/>).

1. Introduction

Diffusion is the slowest transport mechanism in a geological formation. For this reason, in diffusion-dominant systems, groundwater flow is very slow and solute transport is limited. In general, the ratio between advection and diffusion is characterized by the Peclet number ($=vL/D$: v is velocity, L is the characteristic length, D is the diffusion coefficient); diffusion is dominant when the Peclet number is below one. Exploitation of diffusion-dominant domains is considered to be promising for radioactive waste disposal. Therefore, many studies have evaluated diffusion-dominant domains in natural systems. These studies have been summarized [1–3].

In this study, diffusion experiments were conducted to investigate component separation and isotope fractionation by diffusion. The diffusion coefficients of HDO and Cl in free water were investigated [4,5]. The diffusion coefficients of HDO and Cl were similar to that of free water. However, in natural rocks, the diffusion coefficient of HDO was about three times higher than those of anions such as Cl⁻ and Br⁻. This was due to interactions

of the anions with negatively charged clay surfaces, which influence the anionic diffusion [2]. Anions are typically restricted to passing thorough pores by diffusion. By using this difference, the diffusion time and boundary condition changes was discussed [6–8].

Cl isotopes are fractionated by diffusion; therefore, $\delta^{37}\text{Cl}$ is an important tool for the identification of a diffusion-dominant domain. Many studies have attempted to use isotope fractionation to estimate the diffusion time and boundary condition changes [9–13].

A combination of component separation and isotope fractionation is the most promising method to determine whether a system is diffusion-dominant. In Japan, it is common to find that marine sedimentary rock has been uplifted and flushed by meteoric water. This is a suitable condition under which to assess diffusion-dominant domains in which both component separation and isotope fractionation occur, as normally there is a large difference in HDO and Cl between seawater and meteoric water.

In this study, diffusion experiments were conducted with artificial and natural samples to measure the diffusion coefficients of HDO, Cl and Br, as well as the isotope fractionation factors of ^{37}Cl and ^{81}Br . This was the first attempt to determine Br isotope fractionation factors by diffusion for natural rocks in a laboratory. Effective porosity for each component was also measured. Effective porosity influences the progress of diffusion, which depends on D_e/n_e , where D_e is the effective diffusion coefficient and n_e is the effective porosity. If D_e/n_e is the same for HDO and Cl, component separation does not occur. Therefore, effective porosity was also measured to estimate the progress of diffusion.

2. Experimental Method

2.1. Samples

Porous stone, glass filters, and ceramic disks were used as the artificial samples. For the natural samples, the sedimentary rock of the confined layer of the Great Artesian Basin in Australia and siliceous mudstone from Horonobe in the north of Japan were used.

The artificial samples used were various types of filter for soil tests: the glass filters were sintered glass beads, and the porous stones and ceramic disks were sintered clay particles. The porous stones and glass filters were also bound to natural samples to prevent them from collapsing. Ceramic disks are normally used for soil testing. They are categorized by air entry value, which relates to pore radius. Here, air entry values of 1, 3, 5, and 15 Bar were used.

The confined layer of the Great Artesian Basin was from Richmond and Marree, which are the recharge and discharge areas of the Great Artesian Basin, respectively, that were previously drilled and cored [13]. These belong to the Rolling Down Group and are categorized as mudstone [14]. The formation at Richmond is more consolidated compared to Marree. The porosities of Richmond and Marree are about 25% and 40%, respectively.

The Horonobe siliceous mudstone that was used was from the Koetoi and Wakkanai Formation. The difference between these two geological formations lies in the diagenesis of the mudstone [15]. The Koetoi Formation has not undergone diagenesis, is mainly composed of Opal-A, and has a high porosity ratio of about 60%. The Wakkanai Formation has undergone diagenesis, is mainly composed of Opal-CT, and has a lower porosity ratio of about 40% relative to the Koetoi Formation. These rocks were sampled from the Horonobe Underground Research Laboratory (URL). The boundary between the Wakkanai and Koetoi Formations is at a depth of about 250 m in the Horonobe URL.

2.2. Through-Diffusion Experiment

A through-diffusion experiment was conducted as shown in Figure 1 [16]. The purpose of the experiment was to determine the diffusion coefficients for HDO, Cl, and Br and the fractionation factors for the Cl and Br isotopes. Occasionally, samples of sedimentary rocks crack due to swelling and unloading. In these cases, advection occurs due to density-dependent flow between the low- and high-concentration tanks, and the diffusion flux may be overestimated due to advection. Thus, reverse direction diffusion from the low- to high-concentration tank was also measured. In the experiment, the high-concentration tank

contained HDO, Cl, Br, and NAP. NAP is a fluorescent dye—1-Naphthylamine-4-sulfonic Acid Sodium Salt Tetrahydrate. The low-concentration tank contained Na, NO₃, and δ¹⁸O. NaNO₃ solution was used for the desalinization of rock samples, which was necessary as they contained high NaCl contents in their core. The concentrations of the high- and low-concentration tanks are shown in Table 1.

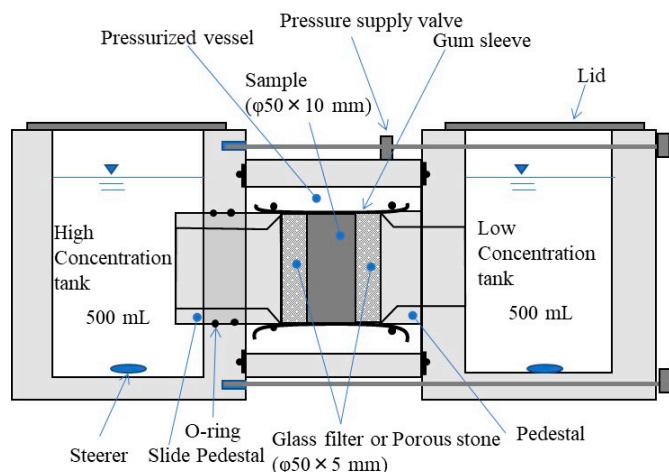


Figure 1. Systematic view of through-diffusion experiment.

Table 1. Tracers used for through-diffusion experiment.

Tracer	Unit	High	Low
HDO	δ ² H (‰ VSMOW)	23,000	−65
H ₂ ¹⁸ O	δ ¹⁸ O (‰ VSMOW)	−13.2	1000
Na		0	28,000
NO ₃		0	74,000
Sr		29,000	0
Cl	mg/L	24,000	0
Cs		8300	0
Br		5000	0
NAP		10	0

The through-diffusion experiment was successful when the diffusion coefficients of δ¹⁸O and NO₃[−] were in agreement with those of HDO and the anions (Cl[−] and Br[−]). The ceramic disks were the same as the samples tested [16]. Porous and glass filters have high conductivity and agar gel was thus used to prevent advective flow [17]. Sedimentary rock may become cracked by swelling. The sedimentary rock samples were thus bound by porous stones or porous glass for structural support, and the high-concentration solutions (Table 1) were used to prevent swelling.

The through-diffusion experiment was conducted as follows:

- (1) Form sample to dimensions of about φ50 mm × H 10 mm.
- (2) Desalinization; dip the sample into NaNO₃ solution.
- (3) Set the sample on the apparatus shown in Figure 1.
- (4) Pour 500 mL of background solution into the low-concentration tank and check that there is no flow.
- (5) Pour 500 mL of tracer into the high-concentration tank.
- (6) Sample 2 mL of solution from the low- and high-concentration tanks every few days.
- (7) Increase the amount of sampling solution to 20 mL for isotope measurement when the Cl concentration is higher than a few hundred mg/L.

(8) End the experiment after taking samples approximately ten times.

Step 2 took about four weeks and was repeated two or three times to confirm the low Cl concentrations. Step 4 was performed to check for cracking by establishing if a flow was present. Step 7 was to measure Cl isotopes, which require at least 3 mg Cl.

2.3. Effective Porosity Experiment

Effective porosity (n_e) is a measure of the accessible porosity of each component, such as HDO, Cl, Br, and NAP [2]. HDO can propagate better than Cl because clay surfaces are normally negatively charged and influence the progress of diffusion of negatively charged ions. Therefore, it is important to determine the effective porosity.

The effective porosity experiment was conducted as follows:

- (1) Dip the sample into the high-concentration solution containing HDO, Cl, Br, and NAP.
- (2) Sample from the high-concentration solution after the concentration stabilizes.
- (3) Remove the sample and dip it into the low-concentration solution
- (4) Sample from the low-concentration solution after the concentration stabilizes.
- (5) Remove the sample and measure its weight when saturated.
- (6) Dry the sample in an oven at 110 °C for 24 h and measure the dry weight.

The effective porosity was calculated as follows:

$$V_C = \frac{V_L C_L}{C_H - C_L} \quad (1)$$

$$n_e = \frac{V_C}{V_S} \quad (2)$$

where V_C is the pore volume of each component, V_L is the solution volume for the low-concentration solution, and C_H and C_L are the concentrations of the high- and low-concentration solutions at Steps 2 and 4, respectively. n_e is the effective porosity, and V_S is the volume of the sample, which can be calculated from the diameter and width.

2.4. Measurements

In this study, HDO (δD), $H_2^{18}O$ ($\delta^{18}O$), Na, Cl, Br, NO_3 , NAP, $\delta^{37}Cl$, and $\delta^{81}Br$ were measured.

δD and $\delta^{18}O$ were determined using cavity ring down spectroscopy (Los Gatos Research, San Jose, CA, USA). The Na^+ , Cl^- , and NO_3 concentrations were determined using ion chromatography (Metrohm Co., Herisau, Switzerland). Inductively coupled plasma mass spectrometry (ICP-MS) was used to determine Br^- content (Agilent Technology, California, US). NAP was determined by fluorescence spectrophotometry (Nihonbunko, Tokyo, Japan).

$\delta^{37}Cl$ and $\delta^{81}Br$ were determined by gas chromatography continuous flow isotope ratio mass spectrometry (GC-CF-IRMS) at the University of Waterloo [18,19] (Agilent Technologies Inc., Santa Clara, CA, USA; Thermo Fisher Scientific, Bremen, Germany). These measurements required at least 3 mg of Cl and Br, respectively.

3. Experimental Results

3.1. Through-Diffusion Experiment

Figures 2 and 3 show the results of the through-diffusion experiments for artificial samples and natural samples, respectively. The upper figure shows concentration change and lower figure shows isotope ratio change.

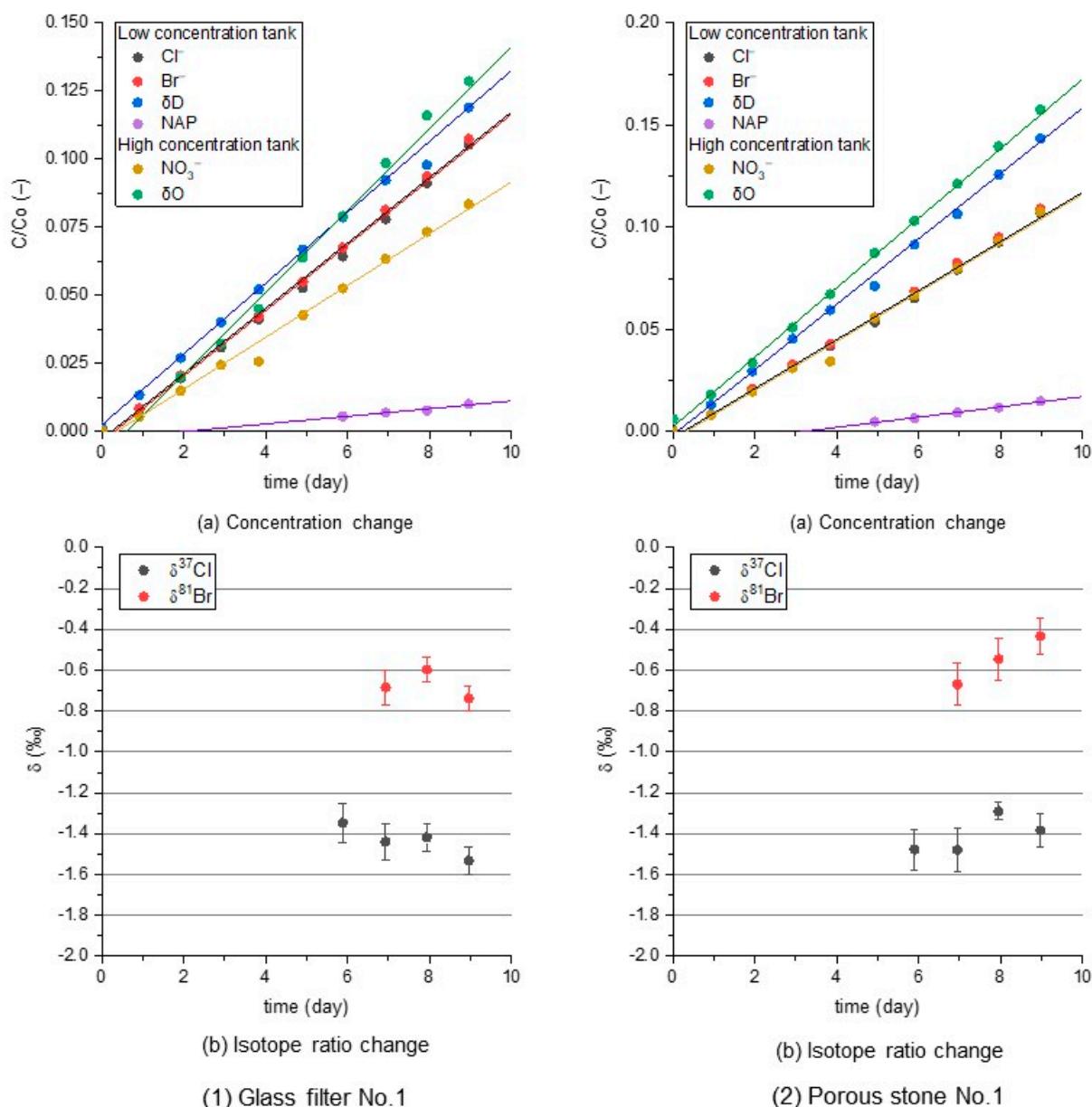


Figure 2. Results of through-diffusion experiment for artificial samples for (1) glass filter No.1 and (2) porous stone No.1, (a) concentration change, (b) isotope ratio change, δ is the difference in the isotope ratio between initial and time series measurements ($\delta = \delta_{t=\text{time}} - \delta_{t=0}$). The absolute value of δ provides the enrichment factor ($(\alpha - 1) \times 1000\%$) if the concentration change effect is neglected.

The results of the through-diffusion experiment are shown in Table 2. The ratios of the diffusion coefficients and isotope fractionation factors are shown in Table 3. The following equation, which transforms the solution for cumulative flux under constrained concentration boundaries [16,20] (pp. 49–53), was used to evaluate the diffusion coefficient:

$$C_{L,t} = \frac{C_{H,0}AW}{V} \left[\frac{D_e t}{W^2} - \frac{n_e}{6} - \frac{2n_e}{\pi^2} \sum_{n=1}^{\infty} \frac{(-1)^n}{n^2} \exp\left(-\frac{D_e n_e n^2 \pi^2 t}{W^2}\right) \right] \quad (3)$$

where $C_{L,t}$ is the concentration in the low-concentration tank at t , t is time, $C_{H,0}$ is the initial concentration in the high-concentration tank, A is the cross-section area in the diffusion

direction of sample, W is the sample width, n_e is the effective porosity, and V is the tank volume. The following approximation can be applied when $D_e t/n_e L^2 > 0.45$ [20] (pp. 49–53):

$$C_{L,t} = \frac{C_H A W}{V} \left[\frac{D_e t}{W^2} - \frac{n_e}{6} \right] \tag{4}$$

The diffusion coefficient can be calculated from the relationship between time and $C_{L,t}$ as follows:

$$D_e = \frac{s V W}{C_H A} \tag{5}$$

where s is the slope between $C_{L,t}$ and t .

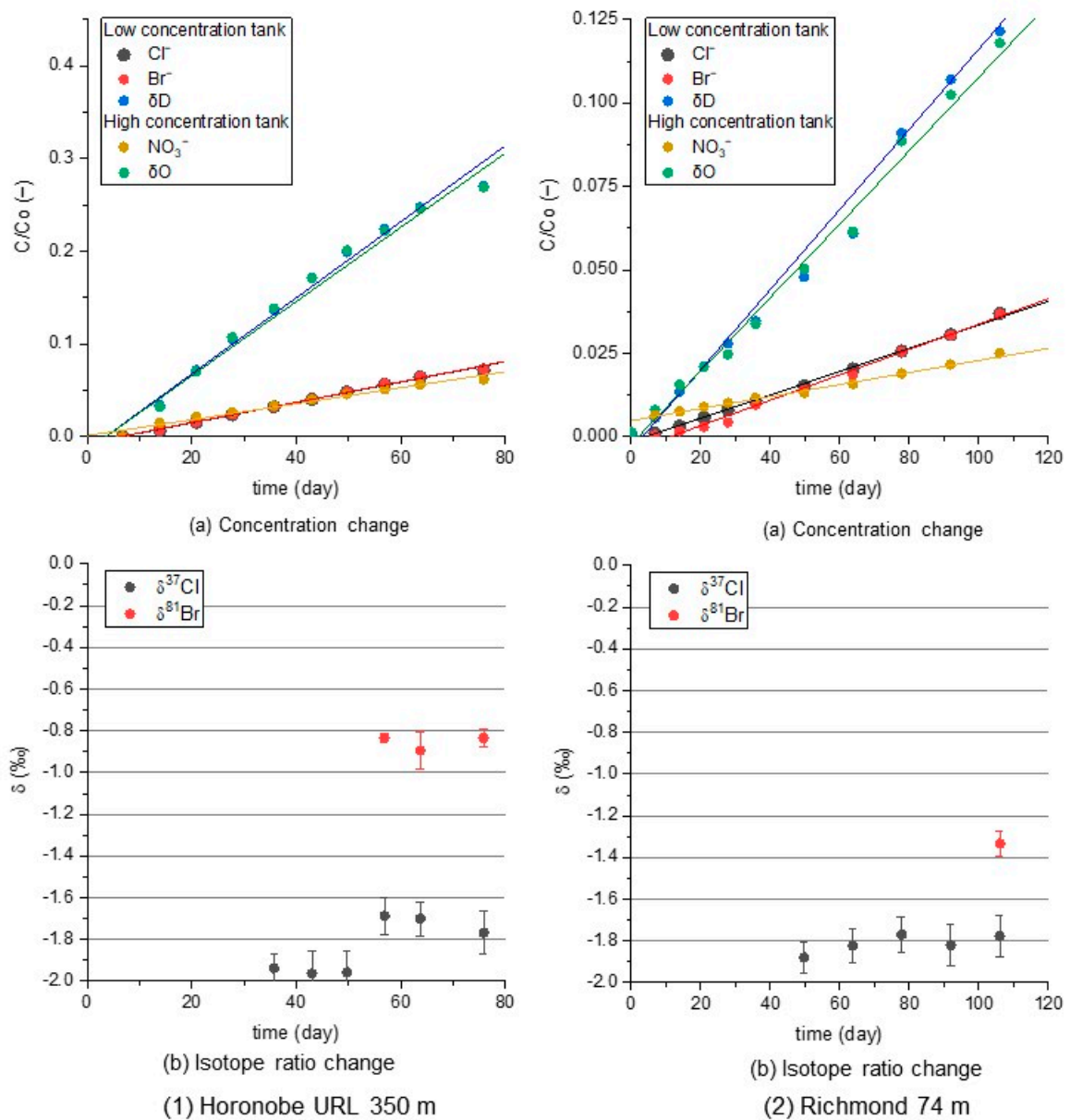


Figure 3. Results of through-diffusion experiment for natural samples or (1) Horonobe URL 350 m and (2) Richmond 74 m, (a) concentration change, (b) isotope ratio change. δ is the difference in the isotope ratio between initial and time series measurements ($\delta = \delta_{t=\text{time}} - \delta_{t=0}$). The absolute value of δ provides the enrichment factor ($(\alpha - 1) \times 1000\text{‰}$) if the concentration change effect is neglected.

Table 2. Diffusion coefficient and fractionation factor by through-diffusion experiment.

Sample Name and Depth			Diffusion Coefficient (m ² /s)					Fractionation Factor							
			Low Concentration Tank				High Concentration Tank		Low Concentration Tank						
			HDO	Cl ⁻	Br ⁻	NAP	δ ¹⁸ O	NO ₃ ⁻	Cl isotope	n	Br isotope	n			
Artificial sample	Ceramic disk	1 Bar	9.3 × 10 ⁻¹¹	8.3 × 10 ⁻¹¹	7.9 × 10 ⁻¹¹	2.1 × 10 ⁻¹¹	N.M.	1.0016	±0.0002	4	1.0007	±0.0000	4		
		3 Bar	6.5 × 10 ⁻¹¹	5.3 × 10 ⁻¹¹	5.0 × 10 ⁻¹¹	9.7 × 10 ⁻¹²		1.0016	±0.0001	4	1.0008	±0.0000	4		
		5 Bar	8.3 × 10 ⁻¹¹	7.1 × 10 ⁻¹¹	7.7 × 10 ⁻¹¹	1.6 × 10 ⁻¹¹		1.0016	±0.0002	4	1.0008	±0.0000	4		
		15 Bar	8.5 × 10 ⁻¹¹	7.4 × 10 ⁻¹¹	8.1 × 10 ⁻¹¹	2.1 × 10 ⁻¹¹		1.0017	±0.0001	4	1.0007	±0.0001	4		
	Glass filter	No. 1	3.7 × 10 ⁻¹⁰	3.5 × 10 ⁻¹⁰	3.6 × 10 ⁻¹⁰	4.1 × 10 ⁻¹¹	4.6 × 10 ⁻¹⁰	2.9 × 10 ⁻¹⁰	1.0016	±0.0001	4	1.0007	±0.0001	3	
		No. 2	3.1 × 10 ⁻¹⁰	2.8 × 10 ⁻¹⁰	2.9 × 10 ⁻¹⁰	3.2 × 10 ⁻¹¹	3.4 × 10 ⁻¹⁰	2.6 × 10 ⁻¹⁰	1.0014	±0.0002	4	1.0009	±0.0002	4	
	Porous stone	No. 1	4.7 × 10 ⁻¹⁰	3.6 × 10 ⁻¹⁰	3.7 × 10 ⁻¹⁰	7.4 × 10 ⁻¹¹	5.1 × 10 ⁻¹⁰	3.7 × 10 ⁻¹⁰	1.0015	±0.0001	4	1.0006	±0.0001	3	
		No. 2	4.8 × 10 ⁻¹⁰	3.6 × 10 ⁻¹⁰	3.7 × 10 ⁻¹⁰	5.9 × 10 ⁻¹¹	4.9 × 10 ⁻¹⁰	3.7 × 10 ⁻¹⁰	1.0016	±0.0001	4	1.0006	±0.0001	3	
Natural sample	Great Artesian Basin, Australia	Richmond	74 m	3.6 × 10 ⁻¹¹	1.1 × 10 ⁻¹¹	1.1 × 10 ⁻¹¹	N.D.	3.3 × 10 ⁻¹¹	5.7 × 10 ⁻¹²	1.0019	±0.0000	5	1.0014	1	
			134 m	2.3 × 10 ⁻¹¹	5.6 × 10 ⁻¹²	5.5 × 10 ⁻¹²		2.3 × 10 ⁻¹¹	3.3 × 10 ⁻¹²	1.0019	±0.0001	5	1.0007	1	
		Marree	141 m	9.9 × 10 ⁻¹¹	3.0 × 10 ⁻¹¹	2.7 × 10 ⁻¹¹		9.2 × 10 ⁻¹¹	1.9 × 10 ⁻¹¹	1.0021	±0.0001	6	1.0009	±0.0001	2
			167 m	1.1 × 10 ⁻¹⁰	3.3 × 10 ⁻¹¹	3.0 × 10 ⁻¹¹		N.M.	3.3 × 10 ⁻¹¹	1.0022	±0.0001	5	1.0008	±0.0000	5
	Horonobe Underground Research Laboratory, Japan	Koetoi Formation	100 m	1.9 × 10 ⁻¹⁰	6.2 × 10 ⁻¹¹	5.1 × 10 ⁻¹¹		2.8 × 10 ⁻¹⁰	5.4 × 10 ⁻¹¹	1.0018	±0.0002	5	1.0007	±0.0001	5
			150 m	2.1 × 10 ⁻¹⁰	9.2 × 10 ⁻¹¹	8.7 × 10 ⁻¹¹		1.6 × 10 ⁻¹⁰	7.3 × 10 ⁻¹¹	1.0018	±0.0001	5	1.0009	±0.0001	5
			200 m	1.9 × 10 ⁻¹⁰	3.5 × 10 ⁻¹¹	3.3 × 10 ⁻¹¹		1.7 × 10 ⁻¹⁰	3.1 × 10 ⁻¹¹	1.0018	±0.0001	5	1.0009	±0.0002	2
		Wakkanai Formation	250 m	1.7 × 10 ⁻¹⁰	3.7 × 10 ⁻¹¹	3.1 × 10 ⁻¹¹		2.7 × 10 ⁻¹⁰	4.2 × 10 ⁻¹¹	1.0022	±0.0001	4	1.0010	±0.0001	4
			300 m	1.6 × 10 ⁻¹⁰	3.3 × 10 ⁻¹¹	3.1 × 10 ⁻¹¹		1.5 × 10 ⁻¹⁰	4.1 × 10 ⁻¹¹	1.0020	±0.0000	5	1.0007	±0.0001	2
			350 m	1.6 × 10 ⁻¹⁰	3.7 × 10 ⁻¹¹	3.7 × 10 ⁻¹¹		1.6 × 10 ⁻¹⁰	2.6 × 10 ⁻¹¹	1.0020	±0.0001	6	1.0010	±0.0000	3

N.M. and N.D. indicate not measured and not detected, respectively.

Table 3. Ratios of the diffusion coefficients and isotope enrichment factors.

Sample Name and Depth		Cl ⁻ *	Br ⁻ *	NAP *	δ ¹⁸ O *	NO ₃ ⁻ *	β **		
Artificial sample	Ceramic disk	1 Bar	0.89	0.85	0.23	N.M.	0.46		
		3 Bar	0.81	0.77	0.15		0.47		
		5 Bar	0.86	0.93	0.20		0.52		
		15 Bar	0.88	0.96	0.25		0.42		
	Glass filter	No.1	0.94	0.96	0.11	1.24	0.77	0.47	
		No.2	0.90	0.93	0.10	1.07	0.82	0.68	
	Porous stone	No.1	0.76	0.78	0.16	1.09	0.78	0.39	
		No.2	0.75	0.77	0.13	1.02	0.78	0.39	
Natural sample	Great Artesian Basin, Australia	Richmond	74 m	0.29	0.31		0.91	0.16	0.75
			134 m	0.24	0.24		1.01	0.15	0.37
		Marree	141 m	0.30	0.28		0.93	0.19	0.41
			167 m	0.30	0.28		0.00	0.31	0.37
	Horonobe Underground Research Laboratory, Japan	Koetoi Formation	100 m	0.33	0.27	N.D.	1.51	0.29	0.41
			150 m	0.44	0.42		0.76	0.35	0.50
		Wakkanai Formation	200 m	0.18	0.17		0.88	0.16	0.51
			250 m	0.22	0.18		1.56	0.25	0.46
			300 m	0.20	0.20		0.94	0.26	0.35
			350 m	0.23	0.23		0.98	0.16	0.48

* The diffusion coefficient was divided by the diffusion coefficient of HDO. ** β (ratio of isotope enrichment factor) was calculated as $(\alpha_{Br}-1)/(\alpha_{Cl}-1)$. N.M. and N.D. indicate not measured and not detected, respectively.

For the ceramic discs, the diffusion coefficients were $6.5\text{--}9.3 \times 10^{-11} \text{ m}^2/\text{s}$ for HDO, $5.0\text{--}8.3 \times 10^{-11} \text{ m}^2/\text{s}$ for Cl and Br, and $0.97\text{--}2.1 \times 10^{-11} \text{ m}^2/\text{s}$ for NAP.

For the glass filters and porous stone, the diffusion coefficients were $3.1\text{--}4.8 \times 10^{-10} \text{ m}^2/\text{s}$ for HDO, $2.8\text{--}3.7 \times 10^{-10} \text{ m}^2/\text{s}$ for Cl and Br, and $3.2\text{--}7.4 \times 10^{-11} \text{ m}^2/\text{s}$ for NAP.

For the artificial samples, the diffusion coefficients of HDO and the anions (Cl and Br) were almost the same, as shown in Table 3 in which the ratio of the diffusion coefficient normalized by the diffusion coefficient for HDO is provided. The diffusion coefficient of NAP was 10–30% of the other components.

For the natural samples, the diffusion coefficient derived from Equation (5) should be corrected to account for the bound porous stone and porous glass. The correction methods will be discussed below.

For the Richmond samples, the diffusion coefficients were $2.3\text{--}3.6 \times 10^{-11} \text{ m}^2/\text{s}$ for HDO and $0.56\text{--}1.1 \times 10^{-11} \text{ m}^2/\text{s}$ for Cl and Br. For the Marree samples, the diffusion coefficients were $0.99\text{--}1.1 \times 10^{-10} \text{ m}^2/\text{s}$ for HDO and $2.7\text{--}3.3 \times 10^{-11} \text{ m}^2/\text{s}$ for Cl and Br. The diffusion coefficient of Richmond was smaller than that of Marree due to the higher porosity of Marree. The diffusion coefficient of HDO was three to four times higher than those of the anions. The diffusion coefficient of NAP could not be estimated because NAP could not be detected in the low-concentration tank.

For the Horonobe samples, the diffusion coefficients were $1.6\text{--}2.1 \times 10^{-10} \text{ m}^2/\text{s}$ for HDO, and $3.1\text{--}9.2 \times 10^{-11} \text{ m}^2/\text{s}$ for Cl and Br. The diffusion coefficient of HDO was similar for all Horonobe samples. On the contrary, the diffusion coefficients of the Koetoi Formation for Cl and Br were slightly larger than those of the Wakkanai Formation. The diffusion coefficient of HDO was two to five times higher than those of the anions. The diffusion coefficient of NAP could not be estimated, as mentioned before.

3.2. Effective Porosity Experiment

The results of the effective porosity experiments are shown in Table 4. This table shows the effective porosities for HDO, Cl, Br, and NAP and the porosities determined with the drying method. The ratios of the porosities divided by the drying porosities are also shown in Table 4.

Table 4. Porosity derived by solute and drying; porosity ratio divided by drying porosity.

(1) Artificial Sample											
Sample Name	Ceramic Disk				Glass Filter		Porous Stone				
	1 bar	3 bar	5 bar	15 bar	No.1	No.2	No.1	No.2			
Porosity	Cl	31.9%	33.8%	34.0%	33.7%						
	Br	N.M.				N.M.					
	HDO	35.5%	38.4%	37.3%	37.9%						
	Drying	31.5%	35.1%	34.6%	34.4%	30.3%	30.4%	41.4%	42.7%		
Porosity ratio *	Cl	101%	96%	98%	98%						
	HDO	113%	109%	108%	110%			N.M.			
(2) Natural Sample											
Location	Great Artesian Basin, Australia				Horonobe Underground Laboratory, Japan						
	Richmond		Marree		Koetoi Formation			Wakkanai Formation			
Depth (m)	74	134	141.5	163	100.2	150.2	200.2	250.5	301	350	
Porosity	Cl	18.2%	13.8%	32.4%	38.1%	62.5%	62.8%	61.9%	47.2%	43.9%	41.8%
	Br	16.1%	12.2%	29.2%	34.6%	66.1%	60.0%	58.8%	49.6%	41.2%	37.6%
	HDO	32.3%	24.0%	48.0%	53.7%	65.8%	69.0%	67.0%	54.5%	52.6%	50.4%
	Drying	28.9%	21.5%	43.1%	49.0%	60.7%	58.2%	57.6%	48.2%	43.9%	43.2%
Porosity ratio *	Cl	63%	64%	75%	78%	103%	108%	107%	98%	100%	97%
	Br	55%	57%	68%	71%	109%	103%	102%	103%	94%	87%
	HDO	111%	112%	112%	110%	108%	118%	116%	113%	120%	117%

* The porosity ratio was calculated by dividing the porosity by the drying porosity.

For the artificial samples, the porosity of HDO was slightly higher than that of Cl but within 12%, so the porosities of HDO and Cl can be considered to be similar. In contrast, for the Richmond and Marree samples, the porosity ratios of Cl and HDO were about 50% and 70%, respectively. For the Horonobe samples, it was 80–100%. The decreasing ratio was smaller than those for Richmond and Marree.

4. Discussion

4.1. Corrections for Natural Samples Bound by Porous Stone and Glass Filters

Natural samples were bound by porous stones or glass filters to prevent cracking by swelling and unloading. Ceramic discs, glass filters, and porous stones were set onto the pedestal directly, without additional support. Thus, a correction had to be applied to accurately estimate the diffusion coefficients for natural rocks.

Assuming a conceptual model of bound samples as shown in Figure 4, under a steady state, the relationship between flux and the diffusion coefficient is expressed as follows:

$$F = D_1 \frac{\Delta C_1}{\Delta L_1} = D_2 \frac{\Delta C_2}{\Delta L_2} = D_3 \frac{\Delta C_3}{\Delta L_3} \quad (6)$$

$$\Delta C = \Delta C_1 + \Delta C_2 + \Delta C_3 \quad (7)$$

where F is flux, D_i is the diffusion coefficient of the i -th material, ΔC_i is the concentration difference within the i -th material, and ΔL_i is the length of the i -th material.

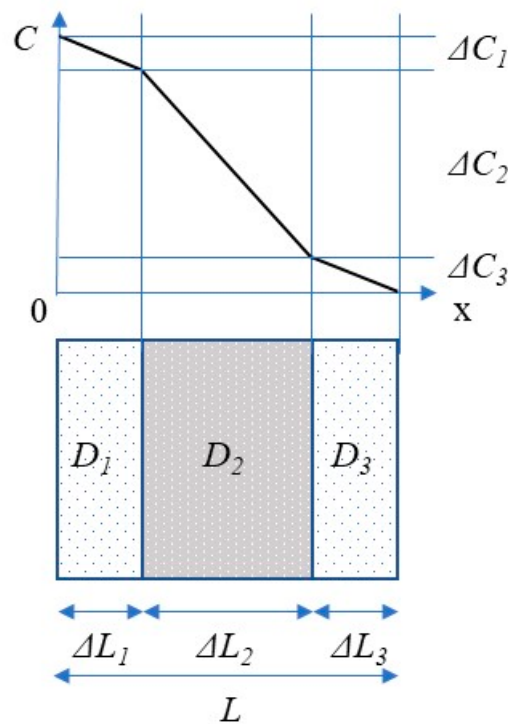


Figure 4. Conceptual model of bound sample.

Considering the experimental condition, $D_1 = D_3$ and $\Delta L_2 = 2\Delta L_1 = 2\Delta L_3$:

$$\Delta C = \Delta C_1 + \frac{D_1 \Delta L_2}{D_2 \Delta L_1} \Delta C_1 + \frac{D_1 \Delta L_3}{D_3 \Delta L_1} \Delta C_1 = 2 \left(1 + \frac{D_1}{D_2} \right) \Delta C_1 \quad (8)$$

$$F = D_1 \frac{\Delta C_1}{\Delta L_1} = \frac{D_1 D_2}{D_2 + D_1} \frac{\Delta C}{\Delta L_2} \quad (9)$$

where the apparent diffusion coefficient D' for length ΔL_2 of the bound sample is as follows:

$$F = D' \frac{\Delta C}{\Delta L_2} = \frac{D_1 D_2}{D_2 + D_1} \frac{\Delta C}{\Delta L_2} \quad (10)$$

Therefore, it becomes the following:

$$D_2 = \frac{D_1 D'}{D_1 - D'} \quad (11)$$

Assuming that the diffusion coefficient for porous stone and glass filters is equivalent to approximately $3 \times 10^{-10} \text{ m}^2/\text{s}$, which is the average of the diffusion coefficient for porous stone and glass filters, the relationship between D_2 and D' is shown in Figure 5. When D_1 is sufficiently larger than D' ($D_1 \gg D'$), D_2 is equivalent to D' ($D_2 \approx D'$).

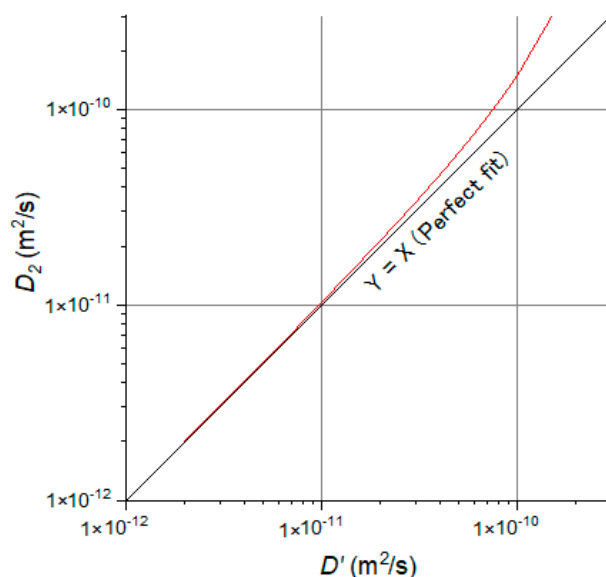


Figure 5. Diffusion coefficient relationship between the bound and target samples. D' on x -axis and D_2 on y -axis are the effective diffusion coefficients for the bounded samples and target sample, respectively. It is assumed that $D_1 = D_3 = 3 \times 10^{-10}$ m/s and $L_2 = 2L_1 = 2L_3$. * D' is calculated for the target sample width (L_2), not for the bounded samples ($L_1 + L_2 + L_3$).

To estimate the isotope fractionation, D_l and D_h are set as the diffusion coefficients for the light and heavy isotopes, respectively. Here, the isotope fractionation factor α is set as D_l/D_h . α' is the isotope fractionation factor of the bounded sample. α' can be expressed as follows:

$$\alpha' = \frac{D'_l}{D'_h} = \frac{\frac{D_{l1}D_{l1}}{D_{l1}+D_{l2}}}{\frac{D_{h1}D_{h2}}{D_{h1}+D_{h2}}} = \frac{D_{l1}D_{l2}(D_{h1} + D_{h2})}{D_{h1}D_{h2}(D_{l1} + D_{l2})} = \alpha_1\alpha_2 \frac{1}{1 + \frac{D_{l2}}{D_{l1}}} + \frac{1}{\alpha_2} \frac{D_{h2}}{D_{h1}} \quad (12)$$

where D_{h2}/D_{h1} and D_{l2}/D_{l1} are equivalent to D_2/D_1 .

As a result, the isotope fractionation factor of α_2 can be solved as follows:

$$\alpha_2 = \alpha' + (\alpha' - \alpha_1) \frac{D_2}{D_1} = \alpha' + (\alpha' - \alpha_1) \frac{D'}{D_1 - D'} \quad (13)$$

Assuming that D_1 and α_1 are set to be 3×10^{-10} m²/s and 1.0014, respectively, α_2 can be calculated by using D' and α' , as shown in Figure 6. When D_1 is significantly larger than D' ($D_1 \gg D'$), α_2 is equivalent to α' ($\alpha_2 \approx \alpha'$). Therefore, if D_1 is significantly larger than D' , D' and α' are equivalent to the original value of D_2 and α_2 .

4.2. Diffusion Coefficient

For the artificial samples consisting of ceramic discs, porous stones, and glass filters, the diffusion coefficients of HDO and Cl were similar. The diffusion coefficients of HDO were about 1.0–1.3 times higher than those of Cl.

On the contrary, for natural samples, the diffusion coefficients of HDO were three to four times higher than those of Cl. The differences in diffusion coefficients for natural samples were much higher than those of artificial samples. This may have been related to the influence of the negative charge of surfaces [21]. The diffusion coefficients of Br were similar to those of Cl. Anions were transported within small areas compared to the water isotopes (HDO and H₂¹⁸O). Thus, the ratio of the diffusion coefficients of HDO and Cl depends on the clay content and pore properties, including the porosity and tortuosity. Thus, a diffusion experiment was necessary to determine the difference in the diffusion coefficients.

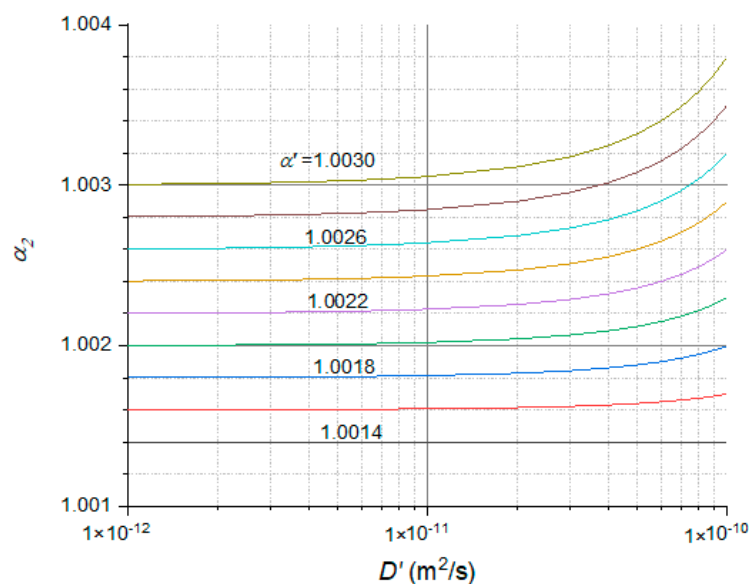


Figure 6. Fractionation factor relationship between bound and target samples. D' on x-axis and α' are the effective diffusion coefficient and fractionation factor for bounded samples, respectively. α_2 on y-axis is the fractionation factor for the target sample. It is assumed that $D_1 = D_3 = 3 \times 10^{-10}$ m/s and $\alpha_1 = \alpha_3 = 1.0014$.

The diffusion coefficient of NAP was about one-fifth that of Cl for artificial samples. In comparison, the diffusion coefficient of natural samples could not be calculated because the NAP concentration in the low-concentration tank was below the analytical detection limit. NAP is organic matter, with a large molecular weight and structure compared to individual ions; thus, it has a very low diffusion coefficient and cannot pass through small pores. If organic matter can be transported by advection and not diffusion, the presence of remaining organic matter relative to other ions may be evidence of a diffusion-dominant domain.

The effective porosity is shown in Table 4. With the exception of the Richmond and Marree samples, there was no significant difference between the effective porosities of HDO and Cl, and all were within 20%. In contrast, in the Richmond and Marree samples, the effective porosity of Cl decreased with a decreasing drying porosity. The ratio of the effective porosities of Cl and HDO was nearly 1.2. It is possible that the difference in the diffusion coefficient was counteracted by the effective porosity. Thus, measuring the effective porosity is important.

As shown above, the diffusion coefficient of HDO was about three to four times higher than that of Cl, and the difference in the effective porosity between HDO and Cl was not significant compared to the difference in diffusion. Therefore, HDO and Cl were separated by diffusion for natural samples but separation did not occur for artificial samples.

4.3. Isotope Fractionation Factor

To estimate the isotope fractionation factor, it was necessary to correct for the initial influence and concentration change [16]. The initial influence could be negated because sampling was not conducted at the beginning of experiment. At least 3 mg of Cl and Br was required to measure these isotopes, so the required volume was too high when the concentration in the solution was low. The effect of concentration change increases with time, so it had to be accounted for. A standard curve was used to correct for this effect [16].

For the through-diffusion experiment, the concentration in the low-concentration tank can be expressed as follows [16], when the initial unsteady state is neglected:

$$C_{L,t} = \frac{1}{\beta} C_{H,0} \left[1 - \exp\left(-\frac{\beta DA}{VW} t\right) \right] \quad (14)$$

where $C_{L,t}$ is the concentration at time t in the low-concentration tank, $C_{H,0}$ is the initial concentration in the high-concentration tank, β is the condition of the high-concentration tank, $\beta = 1$ when the concentration tank remains constant, $\beta = 2$ when the concentration changes (normal condition), D is the diffusion coefficient, A is the sample area, V is the sample volume, W is the sample width, and t is the time, as mentioned before.

Using the above equation, the isotope ratio in the low-concentration tank can be expressed as follows:

$$R_{L,t} = \frac{C_{h,t}}{C_{l,t}} = R_{H,0} \frac{\left[1 - \exp\left(-\frac{\beta D_h A}{VW} t\right)\right]}{\left[1 - \exp\left(-\frac{\beta D_l A}{VW} t\right)\right]} = R_{H,0} \frac{\left[1 - \exp\left(-\frac{\beta D_1 A}{\alpha VW} t\right)\right]}{\left[1 - \exp\left(-\frac{\beta D_1 A}{VW} t\right)\right]} \quad (15)$$

where $C_{l,t}$ and $C_{h,t}$ are the concentration of light and heavy isotopes at t , respectively. α is the fractionation factor ($= D_L/D_H$).

α can be solved as follows:

$$\alpha = -\frac{VWt}{\beta D_1 A} \frac{1}{\ln\left\{1 - \frac{R_{L,t}}{R_{H,0}} \left[1 - \exp\left(-\frac{\beta D_1 A}{VW} t\right)\right]\right\}} \quad (16)$$

Then, the following approximation can be applied:

$$\frac{R_{L,t}}{R_{H,0}} \approx \exp \frac{\delta C_{L,t} - \delta C_{H,0}}{10^3} \quad (17)$$

where Δ is the isotope ratio, subscripts L and H represent the low- and high-concentration tanks, respectively, and subscripts t and 0 represent the time and time = 0 (initial condition), respectively.

α was calculated for each measured value. The α values and associated errors are listed in Table 2 as averages and standard deviations for measured values. For a bound sample, α' can be calculated by Equation (16) and α' can be transformed into α_2 using Equation (13). Here, α_1 is assumed to be the average for glass filters and porous stones. After this, the average and standard deviation can be calculated. α_2 is the fractionation factor of a natural sample.

For artificial samples, the fractionation factor of ^{37}Cl was 1.0016 ± 0.0007 for ceramic disks and 1.0015 ± 0.0001 for porous stone and glass filters. These values were slightly smaller than that of free water, which is 1.0016–1.0018 at 21 °C [17]. The fractionation factor of ^{81}Br was 1.0008 ± 0.0004 for ceramic disks and 1.0007 ± 0.00015 for porous stone and glass filters. These values were similar to that of free water, which is 1.00064 at 21 °C [17]. For the modular dynamics simulation, the fractionation factor was 1.0019 ± 0.0010 for ^{37}Cl [22] and 1.0008 ± 0.0002 for ^{81}Br [23]. The measured fractionation factors for artificial samples were similar to that of free water.

The enrichment factor of ^{81}Br , which was ($\epsilon = (\alpha - 1) \times 1000\%$), was half of that of ^{37}Cl . This was in agreement with the measured value for free water [17].

For natural samples, the fractionation factor of ^{37}Cl was 1.0018 ± 0.00003 for the Koetoi Formation, 1.0020 ± 0.00008 for the Wakkanai Formation, and 1.0020 ± 0.0001 for the Richmond and Marree samples. These fractionation factors were higher than that of free water. The fractionation factors for the Wakkanai Formation were higher than those for the Koetoi Formation. Here, the fractionation factors increased with decreasing porosity. However, the fractionation factors for Richmond were smaller than those for Marree, which does not agree with the trend observed in the Koetoi and Wakkanai formations. This may have been due to influence from the variation in the isotope measurements. The fractionation factor of ^{81}Br was 1.0008 ± 0.00001 for the Koetoi Formation, 1.0009 ± 0.00001 for the Wakkanai Formation, and 1.0008 ± 0.0001 for the Marree and Richmond formations. These values were similar to that of free water and those of artificial samples. The enrichment factors of ^{81}Br were about half of ^{37}Cl , which also agreed with the artificial

samples. There was no significant difference between an artificial and natural sample. The enrichment factor of ^{37}Cl was not as high and the enrichment factor of ^{81}Br did not show a distinct difference.

5. Summary

Through-diffusion experiments and effective porosity experiments were conducted to evaluate diffusion-dominant domains. For these experiments, ceramic discs, porous stones, and glass filters were used as artificial samples. For natural samples, the Koetoi and Wakkanai Formations, which are sedimentary rock formations in Horonobe, Japan, and confined layers sampled at Richmond and Marree in the Great Artesian Basin, Australia, were used.

For the through-diffusion experiments, HDO and H_2^{18}O as water, Cl^- , Br^- and NO_3^- as anions, and NAP as organic matter were used as tracers. It was found that for artificial samples, the diffusion coefficients of water isotopes were only slightly higher than those of the anions Cl^- , Br^- and NO_3^- . The fractionation factor of ^{37}Cl calculated for artificial samples was 1.0014–1.0017, which was equivalent to that of free water. On the contrary, for natural samples, the diffusion coefficient of water isotopes was three to five times higher than for the anions. The fractionation factor of ^{37}Cl calculated for natural samples was 1.0018–1.0021, which is higher than that of free water, as well as that of the artificial samples. This indicates that the negative charge at the surface of the natural samples influences the diffusion coefficient and fractionation factor. The fractionation factor of ^{81}Br was 1.007–1.009 for the artificial samples and 1.007–1.0010 for the natural samples. This was similar to the fractionation factor calculated for free water. The enrichment factor of ^{81}Br was almost half that of ^{37}Cl .

The effective porosity of HDO was larger than for anions, such as Cl^- and Br^- . For natural samples, the coefficient ratio of HDO and the anions was much larger than the effective porosity ratio of HDO and the anions. Therefore, HDO and the anions were separated by diffusion for natural samples. In contrast, HDO and the anions were not separated by diffusion for artificial samples because the diffusion coefficient and effective porosities of HDO and the anions were not so different. Isotope fractionation was observed for all samples; thus, the isotopes of Cl and Br were fractionated by diffusion. The separation of water isotopes and anions and the isotope fractionation of Cl and Br are useful parameters to evaluate whether a domain is diffusion-dominant. An investigation focused on the profile of δD (HDO), Cl, Br, $\delta^{37}\text{Cl}$ and $\delta^{81}\text{Br}$ can play an important role in assessing a diffusion-dominant domain. There are many locations where marine formations have been uplifted and exposed to meteoric water. If this marine formation is in a diffusion-dominant condition, this is a very suitable condition for applying the above method, as seawater and meteoric water have very different δD (HDO) and Cl values, causing a large diffusion gradient. Through-diffusion experiments to estimate the diffusion coefficient and fractionation factors and effective porosity experiments help to better understand diffusion-dominant domains and diffusion times.

Author Contributions: Conceptualization, T.H.; methodology, T.H. and K.N.; investigation, T.H., K.N. and R.G.; writing—original draft preparation, T.H.; writing—review and editing, R.G. All authors have read and agreed to the published version of the manuscript.

Funding: This study entitled ‘Research and development project on high-level radioactive waste disposal in geological formation (Development and Improvement on groundwater flow evaluation technique in rock)’ was supported by the Japanese Ministry of Economy, Trade and Industry (METI). This study is cooperation study between the Central Research Institute of Electric Power Industry and Japan Atomic Energy Agency (JAEA).

Institutional Review Board Statement: Not applicable.

Informed Consent Statement: Not applicable.

Data Availability Statement: Not applicable.

Acknowledgments: We thank T. Tokunaga (University of Tokyo), T. Igarashi (Hokkaido Univ.), S. Takeuchi (Nihon Univ.), T. Yuguchi (Yamagata Univ.), and K. Kashiwaya (Kyoto Univ.) for their advice during this project. The cores of Horonobe were provided by Horonobe Underground Research Center (JAEA). We also thank M. Yoshioka and T. Yamaguchi (Ceres) for experimental support.

Conflicts of Interest: The authors declare no conflict of interest.

References

- Mazurek, M.; Alt-Epping, P.; Gimi, T.; Niklaus Waber, H.; Bath, A.; Gimmi, T. OECD Nuclear Energy Agency. In *Natural Tracer Profiles across Argillaceous Formations: The CLAYTRAC Project*; OECD Nuclear Energy Agency: Paris, France, 2009; 361p.
- Mazurek, M.; Alt-epping, P.; Bath, A.; Gimmi, T.; Waber, H.N.; Buschaert, S.; De Cannière, P.; De Craen, M.; Gautschi, A.; Savoye, S.; et al. Applied Geochemistry Natural tracer profiles across argillaceous formations. *Appl. Geochem.* **2011**, *26*, 1035–1064. [[CrossRef](#)]
- Hendry, M.J.; Solomon, D.K.; Person, M.; Wassenaar, L.I.; Gardner, W.P.; Clark, I.D.; Mayer, K.U.; Kunimaru, T.; Nakata, K.; Hasegawa, T. Can argillaceous formations isolate nuclear waste? Insights from isotopic, noble gas, and geochemical profiles. *Geofluids* **2015**, *15*, 381–386. [[CrossRef](#)]
- Mills, R. Self-diffusion in normal and heavy water in the range 1–45°. *J. Phys. Chem.* **1973**, *77*, 685–688. [[CrossRef](#)]
- Yuan-Hui, L.; Gregory, S. Diffusion of ions in sea water and in deep-sea sediments. *Geochim. Cosmochim. Acta* **1974**, *38*, 703–714. [[CrossRef](#)]
- Rübel, A.P.; Sonntag, C.; Lippmann, J.; Pearson, F.J.; Gautschi, A. Solute transport in formations of very low permeability: Profiles of stable isotope and dissolved noble gas contents of pore water in the Opalinus Clay, Mont Terri, Switzerland. *Geochim. Cosmochim. Acta* **2002**, *66*, 1311–1321. [[CrossRef](#)]
- Pearson, F.J.; Arcos, D.; Bath, A.; Boisson, J.Y.; Fernández, A.M.; Gäbler, H.E.; Gaucher, E.; Gautschi, A.; Griffault, L.; Hernán, P.; et al. *Mont Terri Project—Geochemistry of Water in the Opalinus Clay Formation at the Mont Terri Rock Laboratory—Reports of the Federal Office of Water and Geology (FOWG)*; Geology Series No.5; FOWG: Bern-Ittigen, Switzerland, 2003; ISBN 3-906723-59-3.
- De Craen, M.; Wemaere, I.; Labat, S.; Van Geet, M. *Geochemical Analyses of Boom Clay Pore Water and Underlying Aquifers in the Essen-1 Borehole*; SCK•CEN: Mol, Belgium, 2006.
- Desaulniers, D.E.; Kaufmann, R.S.; Cherry, J.A.; Bentley, H.W. 37Cl-35Cl variations in a diffusion-controlled groundwater system. *Geochim. Cosmochim. Acta* **1986**, *50*, 1757–1764. [[CrossRef](#)]
- Eggenkamp, H.G.M.; Groos, A.F.K. Van Chlorine stable isotopes in carbonatites: Evidence for isotopic heterogeneity in the mantle. *Chem. Geol.* **1997**, *140*, 137–143. [[CrossRef](#)]
- Lavastre, V.; Jendrzewski, N.; Agrinier, P.; Marc Javoy, M.E. Chlorine transfer out of a very low permeability clay sequence (Paris Basin, France). *Geochim. Cosmochim. Acta* **2005**, *69*, 4949–4961. [[CrossRef](#)]
- Rebeix, R.; Le Gal La Salle, C.; Jean-Baptiste, P.; Lavastre, V.; Fourré, E.; Bensenouci, F.; Matray, J.M.; Landrein, P.; Shouakar-Stash, O.; Frapé, S.K.; et al. Chlorine transport processes through a 2000m aquifer/aquitard system. *Mar. Pet. Geol.* **2014**, *53*, 102–116. [[CrossRef](#)]
- Hasegawa, T.; Nakata, K.; Mahara, Y.; Habermehl, M.A.; Oyama, T.; Higashihara, T. Characterization of a diffusion-dominant system using chloride and chlorine isotopes (³⁶Cl, ³⁷Cl) for the confining layer of the Great Artesian Basin, Australia. *Geochim. Cosmochim. Acta* **2016**, *192*, 279–294. [[CrossRef](#)]
- Habermehl, M.A. The great artesian basin. *J. Geol. Soc. Aust.* **1980**, *5*, 9–38. [[CrossRef](#)]
- Ishii, E.; Sanada, H.; Iwatsuki, T.; Sugita, Y.; Kurikami, H. Mechanical strength of the transition zone at the boundary between opal-A and opal-CT zones in siliceous rocks. *Eng. Geol.* **2011**, *122*, 215–221. [[CrossRef](#)]
- Hasegawa, T.; Nakata, K. A measurement method for isotope fractionation of ³⁵Cl and ³⁷Cl by a conventional through-diffusion experiment. *Chem. Geol.* **2018**, *483*, 247–253. [[CrossRef](#)]
- Eggenkamp, H.G.M.; Coleman, M.L. The effect of aqueous diffusion on the fractionation of chlorine and bromine stable isotopes. *Geochim. Cosmochim. Acta* **2009**, *73*, 3539–3548. [[CrossRef](#)]
- Drimmie, R.J.; Shouakar-stash, O.; Drimmie, R.J.; Frapé, S.K. Determination of inorganic chlorine stable isotopes by continuous flow isotope ratio mass spectrometry Determination of inorganic chlorine stable isotopes by continuous flow isotope ratio mass spectrometry. *Rapid Commun. Mass Spectrom.* **2005**, *19*, 121–127. [[CrossRef](#)]
- Shouakar-Stash, O.; Frapé, S.K.; Drimmie, R.J. Determination of Bromine Stable Isotopes Using Continuous-Flow Isotope Ratio Mass Spectrometry. *Anal. Chem.* **2005**, *77*, 4027–4033. [[CrossRef](#)] [[PubMed](#)]
- Crank, J. *The Mathematics of Diffusion*; Oxford University Press: Oxford, UK, 1975. [[CrossRef](#)]
- Van Loon, L.R.; Glaus, M.A.; Mu, W. Anion exclusion effects in compacted bentonites: Towards a better understanding of anion diffusion. *Appl. Geochem.* **2007**, *22*, 2536–2552. [[CrossRef](#)]
- Bourg, I.C.; Sposito, G. Isotopic fractionation of noble gases by diffusion in liquid water: Molecular dynamics simulations and hydrologic applications. *Geochim. Cosmochim. Acta* **2008**, *72*, 2237–2247. [[CrossRef](#)]
- Eggenkamp, H. *The Geochemistry of Stable Chlorine and Bromine Isotopes*; Springer: Berlin/Heidelberg, Germany, 2014; ISBN 9783642285066.